Article | Received 19 September 2024; Accepted 9 December 2024; Published date 19 December 2024
https://doi.org/10.55092/exrna20240017

Influence of radiotherapy on miRNA dynamics in urine extracellular vesicles

Ghadeer Salloum[1], Maria Konoshenko[1], Ekaterina Murina[1], Ilya Ostaltsev[2], Pavel Laktionov[1] and Olga Bryzgunova[1,*]

[1] Institute of Chemical Biology and Fundamental Medicine, Siberian Branch, Russian Academy of Sciences, Novosibirsk 630090, Russia
[2] E.N. Meshalkin National Medical Research Center of the Ministry of Health of the Russian Federation, Novosibirsk 630055, Russia

* Correspondence author; E-mail: olga.bryzgunova@niboch.nsc.ru.

Abstract: Prostate cancer (PCa) is a common malignancy in men, necessitating accurate diagnosis and monitoring to ensure effective treatment and prevent early relapse. Radiation therapy (RT) is a standard treatment for localized PCa, effectively targeting cancer cells. However, predictive markers are required to optimize efficacy and long-term monitoring to mitigate the risks of tumor regrowth and metastasis. This study investigated the levels of 14 miRNAs in urinary extracellular vesicles, comparing healthy individuals (HI) to PCa patients, as well as the dynamics of these miRNA levels 1 month and 3 months post-RT. A high diagnostic potential was detected in 42 miRNA ratios that showed significant differences between HI and PCa patients. Additionally, 43 miRNA ratios exhibited significant changes before RT and at 1 and 3 months post-RT. Aberrant miRNA expression was observed, suggesting their utility as biomarkers for diagnosis and prognosis. Dynamic changes in miRNA expression following RT highlight their potential in assessing treatment efficacy and predicting disease progression. However, evaluating the prognostic value of RT-influenced miRNAs requires long-term patient follow-up and retrospective data analysis.

Keywords: prostate cancer; radiotherapy; miRNA; therapy effectiveness; liquid biopsy; extracellular vesicles; urine

1. Introduction

Recent statistics indicate that cancer remains one of the leading causes of death worldwide, accounting for nearly 10 million deaths in 2020 [1]. Among all cancers, prostate cancer (PCa) is one of the most prevalent in men, ranking second only to lung cancer [2]. Efficient primary diagnosis of PCa, optimized treatment methods, and close monitoring of treatment efficacy—combined with early suppression of metastasis—are essential for effective patient management. Despite significant advancements in molecular biology and imaging, the gold

standard for PCa screening continues to include rectal examination, prostate-specific antigen (PSA) blood tests, and multiparametric magnetic resonance imaging (mpMRI) for local staging [3].

PSA testing fails to determine tumor aggressivity and can result in overdiagnosis, *i.e.*, certain PCa discovered with early detection may develop slowly and may never be life-threatening to the patient. Between 20% and 50% of PCa cases are thought to be overdiagnosed [4]. Despite not being recommended for prostate cancer diagnosis by the U.S. Preventive Services Task Force since 2012 due to issues with overdiagnosis, PSA testing remains in use, particularly for monitoring the recurrence of prostate cancer [5].

Several curative treatment options are available for localized prostate cancer, including radical prostatectomy, radiation therapy (RT), and other ablative procedures [6,7]. RT, also known as radiotherapy, is a crucial component of cancer treatment that utilizes high-energy radiation to eradicate cancer cells and reduce the size of tumors. This treatment modality is employed in various scenarios, including as a primary treatment for cancer and as an adjuvant therapy to eliminate any remaining cancer cells post-surgery [6]. Its precision in targeting cancer cells while minimizing harm to adjacent healthy tissues is a notable strength, making it an effective tool in the fight against cancer [8]. Moreover, radiotherapy's versatility allows it to be utilized in the treatment of a wide spectrum of cancers, ranging from localized tumors to widespread disease [9].

Despite these advantages, radiotherapy has certain limitations. Patients undergoing radiotherapy may experience side effects such as fatigue, skin changes, and potential damage to nearby organs (e.g., the bowels and urinary tract), which can affect their quality of life during treatment [10]. Additionally, there is a risk of long-term effects on healthy tissues, and not all cancer types respond to radiotherapy. Furthermore, some tumors may develop resistance to radiation over time, necessitating alternative treatment strategies [11]. As a result of these processes, 30%–50% of PCa patients treated with RT experience biochemical recurrence (BCR, defined as a PSA level of 0.2 ng/mL or higher) within 10 years post-therapy [12,13].

As a result, patients must undergo a follow-up procedure after treatment, which typically includes regular check-ups and PSA testing every 3–6 months for the first 5 years, followed by annual tests thereafter [14,15]. Therefore, early detection of cancer relapses and tumor growth, along with treatment strategies that prevent metastasis, is crucial for extending patient life and improving quality of life.

In light of the points discussed, it is crucial to identify diagnostic methods for prostate cancer that are less invasive and less painful, yet more accurate than conventional approaches, in order to determine how the cancer will respond to specific treatments.

Extracellular vesicles (EVs), which have garnered significant attention, are a class of membrane vesicles that can be released by any cell type [16,17]. Initially thought of as cellular waste, EVs are now recognized as important mediators of intercellular communication. They play roles in normal physiological processes and contribute to the development of diseases [18,19].

EVs transport several materials from donor to recipient cells, including lipids, RNA species (such as miRNAs, mRNAs, and long non-coding RNAs), oncoproteins, oncopeptides, and DNA fragments. According to newly available data, EVs play critical roles

in the development of cancer. These roles include forming metastasis and creating pre-metastatic niches. It is currently known that cancer cells secrete more EVs than non-cancerous cells. These particles can be extracted from various physiological fluids such as blood, urine, bile, synovial fluid, lacrimal fluid, seminal fluid, ascites, and bronchoalveolar lavage fluids [20,21].

Given that these vesicles are found in urine, which is now widely considered a non-invasive liquid sample (liquid biopsy), urine is increasingly utilized in clinical diagnostics, making it the second most commonly used biofluid after blood [22].

Among the molecules packed into EVs, miRNA holds a prominent position due to its higher prevalence in molar ratio compared to other nucleic acids. It is known for its biological effects and stability, resisting degradation by endogenous RNases [23–25].

miRNAs packed in EVs have been shown to play a role in all key stages of tumor growth, including cell cycle control, apoptosis, angiogenesis, epithelial-mesenchymal transition, invasion, adhesion, DNA repair, metastasis, and others. As a result, their levels vary not only between healthy individuals and patients but also during the development of the disease and during treatment [26,27].

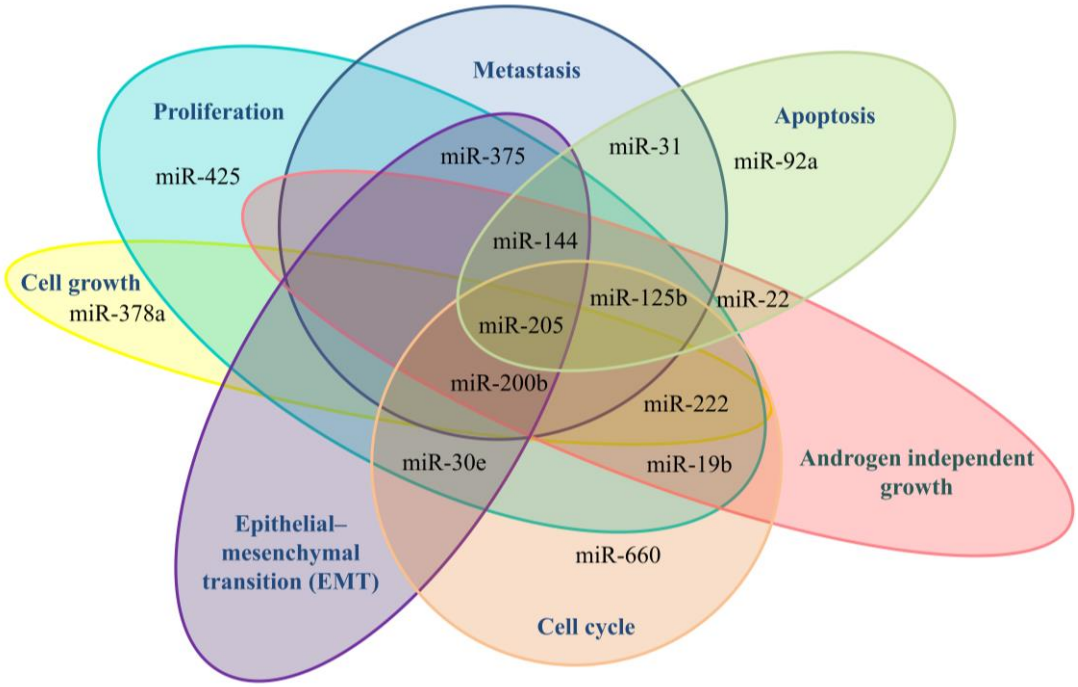

Figure 1. The involvement of the examined microRNAs in different critical biological functions, some of which are disrupted during the course of prostate cancer.

As known, miRNAs play a crucial role in cancer-related processes and are therefore considered important cancer biomarkers [28]. Numerous studies have focused on identifying miRNAs associated with various cancer types [29]. It has been discovered that only 2–8 nucleotides in a miRNA are responsible for binding to the target gene; thus, each miRNA can be able to regulate multiple different genes [30]. However, using miRNAs as biomarkers presents certain challenges, including the need for a reverse transcription step, which requires normalization of expression levels [31]. Initial studies using single miRNAs as unique

markers found that they did not provide sufficient diagnostic value. Instead, it has been shown that sets of miRNAs are more effective for diagnostic purposes [32].

In this study, we aim to investigate the dynamics of 14 miRNA levels in urinary extracellular vesicles (EVs) 1 month and 3 months after RT of PCa patients and to compare them with those in HI.

These microRNAs were selected based on our previously obtained data [33] and taking into account their role in biological processes that are disrupted during the development of prostate cancer (Figure 1).

2. Materials and methods

2.1. Sample collection

The E. N. Meshalkin National Medical Research Center of the Ministry of Health of the Russian Federation (Novosibirsk, Russia) provided urine samples from 17 healthy male individuals (HI) and 17 PCa patients before radiotherapy and after 1 and 3 months post-radiotherapy in accordance with the specific post-therapy follow-up timeline employed at the E. N. Meshalkin National Medical Research Center of the Ministry of Health of the Russian Federation. Table 1 displays the study population's age distribution and mean age, blood PSA levels, disease stage, and Gleason score (for PCa patients). The ICBFM SB RAS ethical committee gave the study its seal of approval (No. 10, 22.12.2008). It is important to mention that all the participants in this study provided a written informed consent.

Table 1. The study populations parameters.

		HI	PCa patients
Age, years	Mean ± standard deviation	54 ± 3.7	62 ± 5.5
	Range	50–60	54–77
Blood PSA, ng/mL	Mean ± standard deviation	0.85 ± 0.1	8.5 ± 0.98
Disease stage	T1N0M0	-	27%
	T2N0M0		73%
Gleason score	5	-	9%
	6		27%
	7		64%

In sterile containers, fresh urine samples were collected. To extract urine supernatant, urogenital tract cells and debris were removed by centrifugation at 400 g for 20 min at room temperature and cleared at 17,000 g for 20 min at 24 ℃.

2.2. Isolation of urinary EVs

The isolation of the EVs was carried out according to the protocol presented by Konoshenko *et al.* [34]. "30 mL of urine supernatant, obtained after centrifugation at 17,000 g, were mixed with 1.25 mL of 1M NaCl, 0.377 mL of PBS, 0.124 mL of 1M Tris-HCl (pH 7.0), 0.1 mL of DEXB (0.1 mg/mL), and 150 mL of PEG solution (25% PEG 20000 in PBS) through repeated pipetting and then incubated for 30 to 40 minutes at 4 ℃." [34]. "The samples were

then centrifuged for 20 minutes at 17,000 g. The supernatant was discarded, and the pellet was resuspended in 3 mL of PBS-like EV fraction, frozen in aliquots in liquid nitrogen, and stored at −80 ℃ for later miRNA isolation." [34].

2.3. Isolation of miRNA by Gu/OcA protocol

The isolation of miRNA from urinary EVs was done as recommended by Lekchnov *et al.* [35]. "EV samples were thawed and gently mixed prior to miRNA isolation. Gu/OcA miRNA isolation from urine. Synthetic cel-miR-39-3p was spiked into the samples at a rate of 5×10^7 copies per isolation after the addition of denaturation buffer. After isolation, each tube received 1.5 µL of glycogen (20 mg/mL, Fermentas) to stabilize the miRNA. 30 µL of RNase-free water were used to dissolve air-dried miRNA pellets." [35].

2.4. Reverse transcription and quantitative RT-PCR

Reverse transcription (RT) on miRNA templates was carried out as described by Chen *et al.* [36]. Medicinal Chemistry Laboratory (ICBFM SB RAS, Novosibirsk) provided the primers and TaqMan probes (see Supplementary Materials, Table S1) for reverse transcription and qPCR. Each RT reaction was performed in a total volume of 10 µL and contained the following ingredients: 2.5 µL of RNA, 25 nM each of miRNA-specific primers (see Table 2), 50 units of M-MuLV-RH reverse transcriptase (Biolabmix, Novosibirsk, Russia), 2 µL of 5×MMLV buffer [250 mM Tris-HCl (pH 8.3 at 25 ℃), 250 mM KCl, 20 mM $MgCl_2$, 50 mM DTT], and 125 mM of each dNTP. The reaction conditions were as follows: 16 ℃ for 30 min, 42 ℃ for 30 min, and 70 ℃ for 10 min. Samples without RNA templates were used as negative controls.

Real-time PCR was carried out using the CFX 96™ Real-Time System from Bio-Rad (USA). A total volume of 24 µL was used for each reaction, which was performed in duplicate. Each reaction contained 4 µL of RT product, 1 unit of Taq DNA polymerase (BiolabMix, Russia), 2.4 µL of 10×PCR buffer (BiolabMix, Russia), 480 nM miRNA-specific forward primer, 640 nM universal reverse primer, and 240 nM specific TaqMan probe (see Supplementary Materials, Table s1). The reactions were conducted for 50 cycles at 95 ℃ for 15 seconds and 60 ℃ for 45 seconds, following an initial denaturation step (95 ℃ for 3 min).

The miRNA expression was evaluated in 2 sets: (miRNA-30e, -19b, -222, -378a, -425, -144, -22, -125b, and cel-miR-39) and (miRNA-30e, -125b, -205, -200b, -375, -19b, -92a, -31, and -660).

2.5. Data analysis and statistical processing

As previously noted, miRNA expression was evaluated in two sets; hence, normalization was only applied within each set (group of miRNAs). Thus, we conducted an examination of 14 miRNAs, resulting in the creation of 61 miRNA ratios (pairs).

Each ratio represents the comparison between two specific miRNAs. To quantify these comparisons, we calculated the Ct difference (dCt) values for each pair of miRNAs as previously stated in the research conducted by Boeri *et al.* and Landoni *et al.* [37,38].

Furthermore, we calculated the dCt difference values (ddCt) between the studied miRNA pairs for both patients after therapy and HI. The ddCt values serve as a measure of the relative expression levels between the miRNA pairs, providing valuable insights into the differences observed between PCa patients and HI.

The statistical analysis was performed using the package provided by GraphPad Prism 8.0. Ratio-based normalization was carried out using Ct values, which evaluated the relative expression of all conceivable combinations of each two miRNAs in the sample.

Depending on the outcome of a normality test, the comparison between groups was made using a one-way ANOVA test or a non-parametric statistical analysis, while a repeated measures statistical test was used to follow the miRNA levels in a single patient.

Receiver operating characteristic (ROC) curves were used to evaluate the analytical system's specificity and sensitivity. The diagnostic efficacy of miRNA ratios was assessed using the area under ROC curves (AUC).

3. Results

It was shown that the assays performed for all miRNAs had a functional range between 24–38 Ct of PCR. RNA samples that produced Ct values within the system's operating range were used to get all of the reported results. It is important to note as well that the spike-in control (cel-miR-39) was detected in all samples at 25 ± 1 Ct.

3.1. The diagnostic characteristics of the studied miRNAs

The expression of 42 miRNA ratios in urinary EVs differed between PCa patients and HI. Table 2 presents the results of comparative expression analysis for miRNA ratios in urinary EVs between PCa patients and HI. Only statistically significant differences are shown. Figure S1 demonstrates the box plots and ROC curves of these 42 miRNA ratios.

Table 2. Differentially expressed miRNA pairs between PCa patients and HI.

Line	MiRNA ratios	ddCt	p-value	Line	MiRNA ratios	ddCt	p-value
1	19b/30e	−1.9	*	22	92a/375	−2.4	***
2	19b/31	1.7	*	23	125b/200b	1.7	***
3	19b/125b	−1.0	*	24	125b/205	1.0	**
4	19b/375	−1.8	*	25	125b/660	0.6	**
5	19b/144	−2.8	***	26	200b/660	−1.1	***
6	19b/222	1.6	**	27	200b/375	−2.5	***
7	19b/378a	1.5	**	28	205/375	−1.8	**
8	19b/425	1.7	***	29	22/144	−4.7	***
9	30e/31	1.4	***	30	22/30e	−2.4	**
10	30e/92a	2.6	***	31	22/125b	−1.4	**
11	30e/200b	2.6	***	32	144/222	4.5	***
12	30e/205	1.9	***	33	144/378a	5.0	***
13	30e/660	1.5	**	34	144/425	5.2	***
14	31/92a	1.1	***	35	144/30e	2.3	*
15	31/125b	−2.8	***	36	144/125b	2.7	***
16	31/200b	−1.1	***	37	222/30e	−2.8	***

Table 2. *Cont.*

Line	MiRNA ratios	ddCt	p-value	Line	MiRNA ratios	ddCt	p-value
17	31/205	−1.7	***	38	222/125b	−1.8	***
18	31/660	−2.2	***	39	378a/30e	−2.7	**
19	31/375	−3.5	***	40	378a/125b	−1.7	***
20	92a/125b	−1.7	***	41	425/30e	−2.9	***
21	92a/660	−1.1	**	42	425/125b	−1.9	***

Aberrant miRNA expression is shown as differences between mean dCt of PCa patients and HI (ddCt); *** $p < 0.001$; ** $p < 0.01$; * $p < 0.05$; t-student test.

A correlation analysis using Pearson's criteria was made to reveal a possible correlation between miRNA ratios and the clinicopathological characteristics of the studied donor groups (Table 3). Only weak (|k|=0.1–0.5) and moderate (|k|=0.5–0.7) correlations with age and PSA were found according to the Cheddok scale. The Pearson correlation coefficient between age and PSA was 0.67 ($p < 0.001$).

Table 3. The results of Pearson correlation analysis between miRNA ratios and clinical-pathological characteristics of studied donors.

Age			PSA		
miRNA ratio	**Pearson coefficient**	**p-value**	**miRNA ratio**	**Pearson coefficient**	**p-value**
19b/31	0.36	*	19b/31	0.37	*
19b/375	−0.36	*	19b/375	−0.34	*
30e/31	**0.51**	***	**30e/31**	**0.67**	**
30e/92a	0.4	*	**30e/92a**	**0.51**	***
30e/200b	0.49	***	**30e/200b**	**0.55**	***
30e/205	0.32	*	30e/205	0.44	*
30e/660	0.3	*	30e/660	0.37	*
31/92a	−0.39	*	**31/92a**	**−0.59**	***
31/125b	**−0.55**	***	**31/125b**	**−0.66**	***
31/205	−0.45	**	**31/200b**	**−0.53**	**
31/660	−0.37	*	**31/205**	**−0.54**	**
31/375	**−0.55**	***	**31/660**	**−0.51**	**
92a/125b	−0.37	*	**31/375**	**−0.63**	***
92a/375	**−0.52**	***	**92a/125b**	**−0.57**	***
125b/200b	0.47	**	**92a/375**	**−0.54**	**
125b/375	−0.32	*	**125b/200b**	**0.62**	***
200b/660	−0.34	*	125b/205	0.41	*
200b/375	**−0.5**	***	**125b/660**	**0.51**	**
205/375	−0.39	*	**200b/375**	**−0.52**	**
660/375	−0.38	*	205/375	−0.44	*
19b/22	0.32	*	660/375	−0.39	*
19b/144	−0.36	*	19b/144	−0.52	**
19b/222	0.45	**	19b/222	0.46	*
19b/425	**0.56**	***	**19b/425**	**0.57**	***
22/144	**−0.59**	***	**22/144**	**−0.6**	***
22/30e	−0.36	*	22/125b	−0.36	*
22/125b	−0.42	**	**144/222**	**0.67**	***
144/222	**0.66**	***	**144/378a**	**0.62**	***
144/378a	0.45	**	**144/425**	**0.68**	***
19b/425	**0.56**	***	**19b/425**	**0.57**	***
22/144	**−0.59**	***	**22/144**	**−0.6**	***
22/30e	−0.36	*	22/125b	−0.36	*

Table 3. *Cont.*

Age			PSA		
miRNA ratio	**Pearson coefficient**	**p-value**	**miRNA ratio**	**Pearson coefficient**	**p-value**
22/125b	−0.42	**	**144/222**	**0.67**	***
144/222	**0.66**	***	**144/378a**	**0.62**	***
144/378a	0.45	**	**144/425**	**0.68**	***
144/425	**0.64**	***	144/30e	0.42	*
144/30e	0.33	*	**144/125b**	**0.56**	***
144/125b	0.38	*	**222/30e**	**−0.52**	**
222/378a	−0.3	*	**222/125b**	**−0.62**	***
222/30e	**−0.58**	***	378a/30e	−0.4	*
222/125b	**−0.51**	***	378a/125b	−0.45	*
378a/425	0.3	*	**425/30e**	**−0.55**	**
378a/125b	−0.3	*	**425/125b**	**−0.58**	***
425/30e	**−0.57**	**			
425/125b	**−0.64**	***			

Moderate correlations are highlighted in bold.

3.2. The dynamics of miRNA expression in urine EVs after RT

In our work, miRNA expre ssion levels in urine EVs from PCa patients before radiotherapy, as well as 1 and 3 months post-radiotherapy, were studied and compared with miRNA expression in urine EVs from healthy individuals. After analyzing the data among 61 ratios, 43 miRNA ratios demonstrated significant changes in the studied timeline.

1 month after RT, miRNA levels differed compared to their levels before RT, and we noticed the formation of three miRNA ratio groups according to the direction of change regarding the normal state (healthy individuals).

The first group (Figure 2A,B) includes 27 miRNA ratios with dCt values that significantly changed 1 month later after radiation towards the bulk of the normal state: 30e/200b, 125b/31, 30e/31, 30e/92a, 30e/378a, 30e/425, 30e/205, 30e/222, 30e/19b, 30e/660, 30e/144, 125b/92a, 200b/660, 425/144, 125b/200b, 222/144, 222/125b, 19b/222, 425/125b, 378a/144, 144/125b, 378a/125b, 19b/378a, 19b/144, 31/660, 205/31, 92a/660. Most of the studied miRNAs (except miR-22 and miR-375) took part in the ratios in this group.

Another group (Figure 2C,D) includes 7 miRNA ratios that did not significantly change 1 month after RT, although significant differences were observed after 3 months (Table 4): 19b/425, 125b/205, 125b/375, 200b/19b, 375/19b, 375/660, and 19b/92a.

The third group (Figure 2E,F) contains 3 miRNA ratios whose ΔCt values after 1 month significantly changed in the opposite direction compared to the healthy donors: 30e/375, 378a/425, and 425/222.

We could not assign six pairs of miRNAs, four of which included miRNA-22, to any of the above groups (Figure 3).

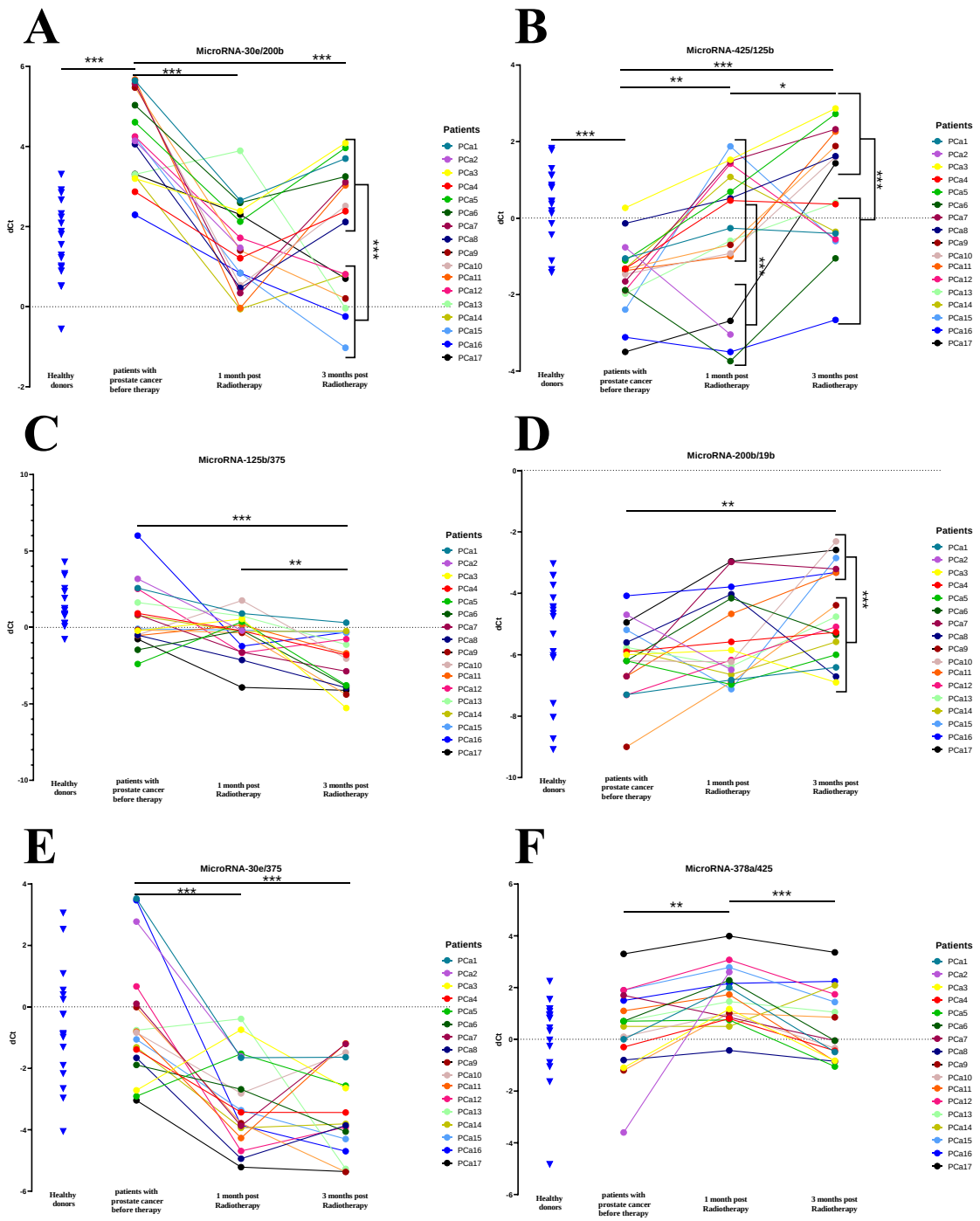

Figure 2. Dynamics of the pairs of prognostic ratio expression (dCt) in urine microvesicles of PCa patients: (**A**, **B**)—miRNA-30e/200b and 425/125b, an example of the 1st group miRNAs (significantly changed 1 month later after radiation towards the normal state); (**C**, **D**)—miRNA-125b/375 and 200b/19b, an example of the 2nd group miRNAs (expressions did not significantly change 1 month after RT (but, looking ahead, there were significant differences after 3 months)); (**E**, **F**)—miRNA-30e/375 and 378a/425, an example of the 3rd group miRNAs (significantly changed after 1 month in the opposite direction in comparison with the healthy donors). «*»—$p < 0.05$, «**»—$p < 0.01$, «***»—$p < 0.001$.

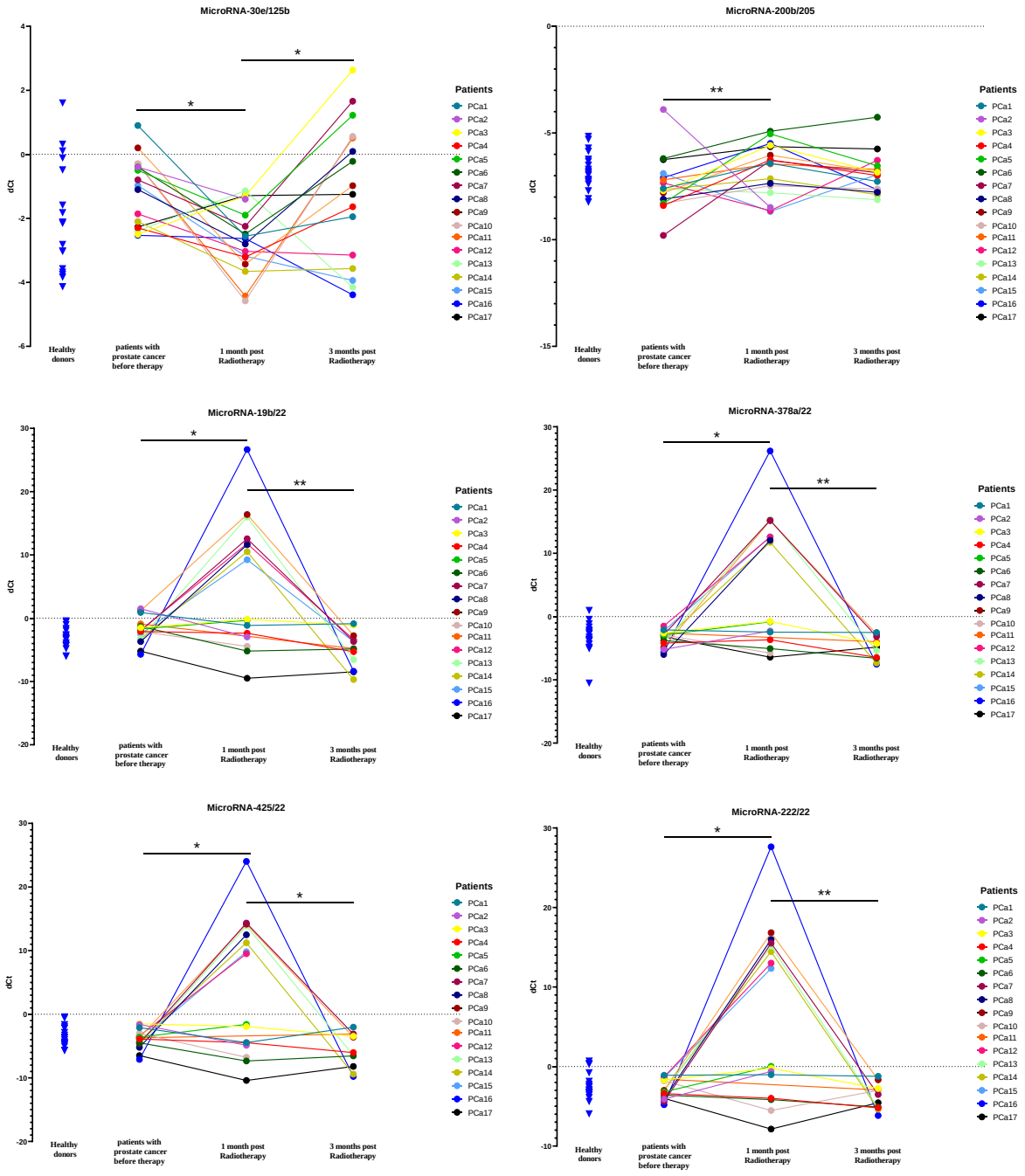

Figure 3. Dynamics of the pairs of prognostic ratio expression (dCt) in urine microvesicles of PCa patients not included in any of the described groups (19b/22, 425/22, 30e/125b, 200b/205, 378a/22, 222/22). «*»—$p < 0.05$, «**»—$p < 0.01$.

Table 4. ddCt mean values for differentially expressed miRNA pairs before and after 1 and 3 months post-radiotherapy.

Line	miRNA ratios	After 1 month post radiotherapy		After 3 months post radiotherapy	
		ddCt	p-value	ddCt	p-value
1	30e/125b	−1.5	*	0.04	-
2	30e/200b	−3.0	***	−2.7	***
3	30e/205	−1.8	**	−1.7	**
4	30e/375	−2.5	***	−2.8	***

Table 4. *Cont.*

Line	miRNA ratios	After 1 month post radiotherapy		After 3 months post radiotherapy	
		ddCt	p-value	ddCt	p-value
5	30e/19b	−2.1	***	−0.9	-
6	30e/92a	−2.4	***	−2.2	***
7	30e/31	−2.8	***	−1.9	***
8	30e/660	−1.4	***	−0.7	-
9	125b/200b	−1.3	**	−2.5	***
10	125b/205	−0.2	-	−1.7	***
11	125b/375	−1.0	-	−2.8	***
12	125b/92a	−0.8	*	−2.3	***
13	125b/31	−1.3	**	−2.0	***
14	200b/205	1.1	**	0.7	-
15	200b/19b	0.7	-	1.6	**
16	200b/660	1.4	***	1.7	***
17	205/31	−1.0	*	−0.3	-
18	375/19b	0.4	-	1.9	**
19	375/660	1.1	-	2.0	**
20	19b/92a	−0.3	-	−1.3	**
21	92a/660	0.9	*	1.5	***
22	31/660	1.4	**	1.2	*
23	30e/378a	−3.2	***	−1.7	**
24	30e/425	−2.3	***	−1.9	***
25	30e/222	−3.5	***	−2.1	**
26	30e/144	3.2	**	2.0	-
27	19b/378a	−1.5	**	−1.4	**
28	19b/425	−1.6	-	−3.8	**
29	19b/222	−1.8	**	−1.8	**
30	19b/144	4.8	***	2.3	**
31	19b/22	8.6	*	−2.9	-
32	378a/425	0.9	**	−0.2	-
33	378a/144	6.4	***	3.9	***
34	378a/22	10.3	*	−1.4	-
35	378a/125b	2.2	***	2.1	***
36	425/222	−1.2	**	−0.2	-
37	425/144	5.4	***	4.0	***
38	425/125b	1.3	**	2.3	***
39	425/22	9.2	*	−1.6	-
40	222/144	6.7	***	4.3	***
41	222/22	10.4	*	−0.9	-
42	222/125b	2.5	***	2.5	***
43	144/125b	−4.3	***	−1.7	-

miRNA expression dynamics is shown as differences between mean dCt before RT and after 1, 3 months of RT, *** $p < 0.001$; ** $p < 0.01$; * $p < 0.05$; ANOVA repeated measures with "Bonferroni's Multiple Comparison Test".

3 months after RT (Table 4), the miRNA ratios mostly maintained the same general dynamics, but with some difference: miRNA-30e/19b, 125b/375, 205/31, 375/19b, 375/660 and 19b/144 joined the third group and started moving opposite to HI; miRNA ratios 125b/205, 200b/19b and 19b/425 joined the first group and started moving towards HI; miRNA ratios 19b/92a, 30e/378, 30e/222, 30e/144, 30e/660, 222/144, 425/144, 378a/144, 378a/425, 144/125b and 425/222 were divided into two subgroups in different directions relative to the 1 month point, but all values still remained "within the HI group"; and miRNA ratios 30e/125b, 200b/205, 378a/22, 425/22, 19b/22, 222/22 have lost their prognostic properties.

In Table 5, we summarize what we mentioned above and show the final sorting of the miRNA pairs according to their dynamics after 3 months post-RT.

Table 5. The changes in miRNA expression profile after 3 months' post-radiotherapy.

Groups according to the direction of change regarding the normal state	MicroRNA ratios
Group 1: 19 miRNA ratios that significantly changed 3 months later after RT towards the normal state (Figure 1B)	30e/200b, 30e/205, 30e/92a, 30e/31, 125b/200b, 125b/205, 125b/92a, 125b/31, 200b/19b, 200b/660, 92a/660, 31/660, 30e/425, 19b/378a, 19b/222, 378a/125b, 425/125b, 222/125b, 19b/425
Group 2: 7 miRNA ratios that changed in the opposite direction in comparison with the healthy individuals	30e/375, 30e/19b, 125b/375, 205/31, 375/19b, 375/660, 19b/144
Group 3: 11 miRNA ratios that divided into two subgroups in different directions relative to the 1-month point, but all values still remained "within the HI group" (Figure 2A)	30e/660, 19b/92a, 30e/378a, 30e/222, 30e/144, 378a/425, 378a/144, 425/222, 425/144, 222/144, 144/125b

4. Discussion

MiRNAs are associated with proliferation, apoptosis, and the regulation of cell fate. In addition to these essential functions, miRNAs are connected to a variety of physiological processes, including immunological responses [39]. Thus, the profiling of miRNA expression in cancer has been useful in determining the etiological significance of particular miRNAs related to cancer initiation, development, and/or metastasis, as well as in identifying differentially expressed miRNAs that may have diagnostic, prognostic, and/or predictive potential [40–42].

Building on the findings mentioned above, this article investigates the expression levels of 14 miRNAs, arranged into 61 ratios, in urine EVs obtained from healthy males and PCa patients (both before and after radiotherapy).

Our analysis identified notable differences in the expression levels of 42 miRNA pairs between healthy individuals and PCa patients. Based on the results of correlation analysis with clinicopathological characteristics (Table 3), we can conclude that our proposed analysis of these 14 miRNAs demonstrates potential for universal applicability. 14 of these ratios (Table 6) exhibited the highest levels of sensitivity and specificity with the highest diagnostic potential (AUC > 0.9). Notably, the miRNA-30e/31 ratio achieved the highest AUC value, amounting to 1.000.

Table 6. miRNA ratios with the best diagnostic performance.

Line	miRNA ratios	AUC	Line	miRNA ratios	AUC
1	30e/31	1.000	8	425/125b	0.912
2	30e/92a	0.935	9	125b/200b	0.971
3	30e/200b	0.951	10	19b/425	0.905
4	222/125b	0.954	11	22/144	0.928

Table 6. *Cont.*

Line	miRNA ratios	AUC	Line	miRNA ratios	AUC
5	31/125b	0.964	12	144/222	0.967
6	92a/125b	0.940	13	144/378a	0.931
7	425/30e	0.913	14	144/425	0.984

The obtained results are consistent with known literature databases and agree with what's mentioned in them. For example, two miRNA pairs (200b/30e, 30e/31) from the ones that demonstrated the highest levels of sensitivity and specificity above were also mentioned in a previous study [43].

It was shown that the chosen miRNAs take a role in the occurrence and progression of prostate cancer. For example, studies have reported that the levels of miRNA-125b [44,45] and miRNA-222 [46,47] differ between prostate cancer patients and healthy donors [48], as do the levels of miRNA-19b [49], miRNA-92a [50], miRNA-200b [33], and miRNA-31 [51]. These findings highlight the potential of these miRNAs as biomarkers for the diagnosis and prognosis of prostate cancer. Therefore, we decided to continue monitoring these miRNAs in the same patient group at 1 and 3 months after radiotherapy.

Radiotherapy has long been recognized for its benefits in treating cancer. However, radiation-induced damage to nearby normal tissues due to direct radiation exposure, or the so-called "bystander effect", which refers to biological consequences in non-irradiated cells brought on by signals from irradiated cells, remains a concern [52]. Individual chemical bonds are broken when high-energy ionizing radiation particles enter the body and release electrons from atoms and molecules. This produces very reactive ions and ion pairs that are often referred to as reactive oxygen species (ROS). It has been suggested that most RT-induced cellular genetic damage is caused by ROS [53].

The phenomenon known as the "radiation-induced bystander effect" describes how signals from neighboring irradiated cells cause non-irradiated cells to exhibit effects at varying levels. Non-irradiated cells may respond by altering processes such as gene expression, translation, cell proliferation, apoptosis, and cell death [54]. In other words, radiotherapy affects the expression of miRNA in addition to the release of extracellular vesicles, thus the miRNA levels.

All the complications mentioned above affect the miRNA profile. These complications can be acute (cell deaths and inflammation). This is why we decided to test at the one-month point after radiotherapy to give the organism a chance to heal because the necrosis or apoptosis of cells will introduce noise, which will affect our results and make them hard to explain. Complications can also last for a long time, like fibrosis, for example, which is believed to be a long-term complication of radiotherapy [55].

Determining the impact of radiotherapy on the expression of the 14 studied miRNAs was the primary goal of the current study. Radiotherapy is known to generate multidirectional changes in miRNA relative expression levels and to have a substantial impact on their expression [56–58]. Nevertheless, the literature has only a small number of studies examining modifications in miRNA expression following radiation, particularly in dynamics [59]. Most

studies focus on analyzing the effect of radiotherapy on one point only, whereas we provided the miRNA expression dynamics before and 1 and 3 months' after RT.

According to the obtained results, 43 miRNA ratios demonstrated significant changes in the studied timeline; 19 of them included the miRNAs, whose dynamics either returned to normal (compared to healthy donors) or shifted toward the normal profile (see Figure 1A, Table 4). These miRNA ratios show high potential in terms of assessing the efficacy of radiotherapy and evaluating and predicting illness progression.

The second group, whose dynamics changed in the opposite direction compared to healthy donors (see Figure 2C, E), may be associated with the side effects of radiotherapy since it is known that radiotherapy can cause several side effects like fibrosis, inflammation, and acute toxicity (gastrointestinal and genitourinary), in addition to the fact that the cell response for such therapy includes different events like oxidative stress, hypoxia, DNA repair, and apoptosis [56,60], and miRNAs are key regulators in all of these events [61,62].

There was a group of miRNA ratios whose dynamics showed minimal change after 1 and 3 months, remaining at the same level with the patients (Figure 2). It is too early to provide a clear explanation for this group. Further monitoring and research will be crucial to giving a better understanding, as their profile may change after 6 months or 1 year, potentially aligning with the first or third group.

It is important to take into account that patients after treatment could not be considered healthy individuals. Thus, some markers can remain dysregulated even after treatment as well as during remission [14,15,56,57].

As for group 2, it is important to note that although we are discussing the direction of ddCt values in an opposite direction to HI, attention should be given to the initial absence of significant differences between HI and the point before RT; therefore, the direction of this group will always be opposite to HI (Figure 1 C–E).

It should be highlighted that there were differences between miRNA pairs with high diagnostic potential and those with the highest prognostic potential. This suggests that the investigated miRNAs have varying potential for diagnosis, prognosis, and relapse prediction and, thus, varied areas of use.

For example, based on the data in Table 3, good prognostic indicators (ddCt values $\geq |2|$ and $p < 0.001$) 3 months after RT were demonstrated by 18 pairs of miRNAs (consisting of 12 miRNAs: -30e, -200b, -375, -92a, -125b, -660, -222, -19b, -425, -144, -378a, and -22), with miRNA-30e, 222, and -144 occurring in four pairs and miRNA-125b in six pairs. These miRNAs may be considered prognostic as soon as their relative expression alters towards HI, whereas no donors with relapse (at the 3-month point) were detected. However, to confirm this conclusion, a longer period of observation is necessary.

Based on the sign of the ddCt values (+ or −, Table 3) and the direction of changes relative to HI (Table 4), we can conclude that miRNA-30e, -125b, and -144 play a tumor-suppressor role, while miRNA-222 appears to have an oncogenic role.

MiRNA-30e is a member of the miRNA-30 cluster. This cluster is consisted of 6 miRNAs (miR-30a, miR-30b, miR-30c, miR-30d, and miR-30e) [63]. The miR-30 cluster is associated with cell differentiation, cellular senescence, and apoptosis. It is also involved in

the pathogenesis of tumors and other disorders of the nervous, genital, circulatory, alimentary, and respiratory systems. [63]. MiRNA-30e is considered a tumor suppressor in different tumors, including PCa. In PCa, miRNA-30e levels are downregulated. If restored, it reduces expression of several mRNAs like androgen receptor, F-Box Protein 45 (FBXO45), Serine and Arginine Rich Splicing Factor 7 (SRSF7), MYB proto-oncogene like 2 (MYBL2), and HELLP-Associated Long Non-Coding RNA (HELLPAR), which play a key role in apoptosis, cell cycle, and ubiquitination [64–66].

MiRNA-125b was mentioned in different studies as a tumor suppressor; thus, it was shown that this particular miRNA plays a crucial role in modulating various signaling pathways, including NF-κB, p53, PI3K/Akt/mTOR, ErbB2, and Wnt. Through these pathways, it can influence processes such as cell proliferation, differentiation, metabolism, apoptosis, drug resistance, and tumor immunity [67,68]. Its expression level was downregulated in various tumors since the low expression of miR-125b promotes cell proliferation, migration, and invasion [69]. In PCa, this miRNA functions as a tumor suppressor. Studies have shown that miRNA-125b levels are markedly reduced in tumor tissues compared to benign prostate tissues in patients [67].

A similar observation was made with microRNA-144. It was downregulated in patients compared to healthy individuals, and since it is known that this microRNA acts as a tumor suppressor, its expression was downregulated in several tumors like lung cancer [70], esophageal squamous cell carcinoma (ESCC) [71], gastric cancer (GC) [72], and also prostate cancer [73,74].

In support of our data, microRNA-222 is a widely studied oncogenic miRNA commonly overexpressed in various human cancers, including esophageal adenocarcinoma, gastric adenocarcinoma, colorectal adenocarcinoma, hepatocellular carcinoma, pancreatic ductal adenocarcinoma [75–77], and prostate cancer [78].

We also mentioned the observation of subgroup formation in some miRNA pairs (for example, 19b/425 and 425/125b at the 1-month point, and 92a/30e, 30e/200b, 31/30e, 378a/30e, and 30e/222 at the 3-month point) (Figure 2). These can be due to various factors; one suggestion can be the radiosensitivity or radiation resistance of the tumor, which can affect the miRNA profile between patients. The largest percentages of microRNAs included in these pairs are miR-30e and 425. In the literature, there is data on changes in miR-425 in the blood plasma of patients with head and neck squamous cell carcinoma (HNSCC) [79] and miR-30e in glioma cells after they received RT [80], but such data could not be found in PCa diseases.

Moreover, several studies have shown that miRNAs (222 [81,82], 31 [83], and 19b [84,85]) are also highly responsible for the radiosensitivity and radiation resistance in different tumors.

Naturally, there are several reasons why it isn't always possible to definitively and properly identify the roles that certain miRNAs play in the development of cancer or before or after therapy. First off, there is the intricate network of interactions between mRNA and miRNA molecules that control their expression. The expression of miRNAs varies in response to a wide range of stimuli since a single miRNA might be engaged in numerous

cascades and processes [86]. Second, there are numerous individual characteristics that might impact the dynamics of the relative expression of any miRNA in a single donor. These include the presence of concomitant disorders (acute and chronic), complications during radiotherapy, drug use, and more. Thirdly, the particulars of the experiment's design, like the type of biomaterial chosen, how it was prepared, and how miRNA expression was assessed, also influence the analysis's findings [87].

5. Conclusion

In conclusion, our investigation into the expression levels of 14 miRNAs in urine EVs from HI and PCa patients, both before and after radiotherapy, has yielded significant insights. Distinct differences in the miRNA expression levels between healthy donors and PCa patients were observed.

The miRNAs examined in this study can be categorized into mostly oncogenic, mostly tumor suppressive, and of unclear function groups. Our findings align with previous studies, indicating the potential of these miRNAs as biomarkers for the diagnosis and prognosis of prostate cancer.

Furthermore, our study tracked the changes in miRNA expression dynamics before radiotherapy and at 1 and 3 months post-radiotherapy. We identified two main groups of miRNA pairs based on their dynamic profiles. In our view, the most promising miRNA pairs for assessing the effectiveness of radiotherapy are 19 pairs consisting of 11 miRNAs (30e, 200b, 205, 92a, 31, 125b, 19b, 660, 425, 378a, and 222).

Our study sheds light on the intricate and multifaceted interplay between miRNA expression and radiotherapy, emphasizing the potential of miRNAs as biomarkers for assessing treatment response and disease progression in prostate cancer. Nonetheless, the complexities of miRNA expression dynamics and the influence of various factors necessitate continued research to fully elucidate their roles in cancer development and therapy response, particularly in the context of long-term outcomes and potential relapse or metastasis.

Abbreviations

PCa: prostate cancer; PSA: prostate specific antigen; mpMRI: Multiparametric magnetic resonance imaging; RT: radiation therapy; BCR: biochemical recurrence; EVs: Extracellular vesicles; HI: healthy male individuals; RT: Reverse transcription; dCt: Ct difference; ddCt: dCt difference values; ROC: Receiving operator characteristic; AUC: area under ROC curves; ROS: reactive oxygen species.

Supplementary data

The authors confirm that the supplementary data are available within this article. Table S1. Sequences of primers and TaqMan probes used in the current study. Figure S1. the box plots and ROC curves of these 42 miRNA ratios.

Acknowledgments

Funding: Russian Science Foundation, Grant/Award Number: 23-25-10026; Government of the Novosibirsk Region, Grant/Award Number: 000000540699599823512058 2/No. p−45.

Conflicts of interests

The authors declare no conflicts of interest.

Ethical statement

The study was performed in accordance with the Declaration of Helsinki and approved by the ethics committee of ICBFM SB RAS (No. 10, 22.12.2008). Written informed consent was provided by all participants.

Authors' contribution

Conceptualization, O.B., M.K and P.L.; methodology, G.S., M.K., E.M., I.O. and O.B.; formal analysis, G.S.; investigation, G.S.; resources, I.O.; data curation, P.L., E.M. and I.O.; writing—original draft preparation, G.S. and O.B.; writing—review and editing, M.K., P.L., E.M. and I.O..; visualization, G.S. and O.B.; supervision, P.L. and O.B. All authors have read and agreed to the published version of the manuscript.

References

[1] Ferlay J, Colombet M, Soerjomataram I, Parkin DM, Piñeros M, *et al.* Cancer statistics for the year 2020: An overview. *Int. J. Cancer* 2021, 149(4):778–789.

[2] Sung H, Ferlay J, Siegel RL, Laversanne M, Soerjomataram I, *et al.* Global Cancer Statistics 2020: GLOBOCAN Estimates of Incidence and Mortality Worldwide for 36 Cancers in 185 Countries. *CA Cancer J. Clin.* 2021, 71(3):209–249.

[3] Descotes JL. Diagnosis of prostate cancer. *Asian J. Urol.* 2019, 6(2):129–136.

[4] Loeb S, Bjurlin MA, Nicholson J, Tammela TL, Penson DF, *et al.* Overdiagnosis and overtreatment of prostate cancer. *Eur. Urol.* 2014, 65(6):1046–1055.

[5] US Preventive Services Task Force; Grossman DC, Curry SJ, Owens DK, Bibbins-Domingo K, Caughey AB, *et al.* Screening for Prostate Cancer: US Preventive Services Task Force Recommendation Statement. *JAMA* 2018, 319(18):1901–1913.

[6] Hamdy FC, Donovan JL, Lane JA, Mason M, Metcalfe C, *et al.* 10-Year outcomes after monitoring, surgery, or radiotherapy for localized prostate cancer. *N. Engl. J. Med.* 2016, 375(15):1415–1424.

[7] Nguyen-Nielsen M, Borre M. Diagnostic and Therapeutic Strategies for Prostate Cancer. *Semin. Nucl. Med.* 2016, 46(6):484–490.

[8] Reijnen C, Brunenberg EJL, Kerkmeijer LGW. Advancing the treatment of localized prostate cancer with MR-guided radiotherapy. *Prostate Cancer Prostatic Dis.* 2023, 26(1):50–52.

[9] Schaue D, McBride WH. Opportunities and challenges of radiotherapy for treating cancer. *Nat. Rev. Clin. Oncol.* 2015, 12(9):527–540.
[10] Gay HA, Michalski JM. Radiation Therapy for Prostate Cancer. *Mo. Med.* 2018, 115(2):146–150.
[11] Sekhoacha M, Riet K, Motloung P, Gumenku L, Adegoke A, *et al.* Prostate Cancer Review: Genetics, Diagnosis, Treatment Options, and Alternative Approaches. *Molecules* 2022, 27(17):5730.
[12] Lamy PJ, Allory Y, Gauchez AS, Asselain B, Beuzeboc P, *et al.* Prognostic Biomarkers Used for Localised Prostate Cancer Management: A Systematic Review. *Eur. Urol. Focus* 2018, 4(6):790–803.
[13] Descotes JL. Diagnosis of prostate cancer. *Asian J. Urol.* 2019, 6(2):129–136.
[14] May EJ, Viers LD, Viers BR, Kawashima A, Kwon ED, *et al.* Prostate cancer post-treatment follow-up and recurrence evaluation. *Abdom. Radiol. (NY).* 2016, 41(5):862–876.
[15] Mohler JL, Kantoff PW, Armstrong AJ, Bahnson RR, Cohen M, *et al.* Prostate cancer, version 2.2014. *J. Natl. Compr. Canc. Netw.* 2014, 12(5):686–718.
[16] Deatherage BL, Cookson BT. Membrane vesicle release in bacteria, eukaryotes, and archaea: a conserved yet underappreciated aspect of microbial life. *Infect. Immun.* 2012, 80(6):1948–1957.
[17] Robinson DG, Ding Y, Jiang L. Unconventional protein secretion in plants: a critical assessment. *Protoplasma* 2016, 253(1):31–43.
[18] Johnstone RM, Adam M, Hammond JR, Orr L, Turbide C. Vesicle formation during reticulocyte maturation. Association of plasma membrane activities with released vesicles (exosomes). *J. Biol. Chem.* 1987, 262(19):9412–9420.
[19] Colombo M, Raposo G, Théry C. Biogenesis, secretion, and intercellular interactions of exosomes and other extracellular vesicles. *Annu. Rev. Cell Dev. Biol.* 2014, 30:255–289.
[20] Witwer KW, Buzás EI, Bemis LT, Bora A, Lässer C, *et al.* Standardization of sample collection, isolation and analysis methods in extracellular vesicle research. *J. Extracell. Vesicles* 2013, 2(1):20360.
[21] Xu R, Rai A, Chen M, Suwakulsiri W, Greening DW, *et al.* Extracellular vesicles in cancer — implications for future improvements in cancer care. *Nat. Rev. Clin. Oncol.* 2018, 15(10):617–638.
[22] Erdbrügger U, Blijdorp CJ, Bijnsdorp IV, Borràs FE, Burger D, *et al.* Urinary extracellular vesicles: A position paper by the Urine Task Force of the International Society for Extracellular Vesicles. *J. Extracell. Vesicles.* 2021, 10(7):e12093.
[23] Gold B, Cankovic M, Furtado LV, Meier F, Gocke CD, *et al.* Do circulating tumor cells, exosomes, and circulating tumor nucleic acids have clinical utility? A report of the association for molecular pathology. *J. Mol. Diagn.* 2015, 17(3):209–224.
[24] Silva J, García V, Zaballos Á, *et al.* Vesicle-related microRNAs in plasma of nonsmall cell lung cancer patients and correlation with survival. *Eur. Respir. J.* 2011, 37(3):617–623.
[25] Vickers KC, Palmisano BT, Shoucri BM, Shamburek RD, Remaley AT. MicroRNAs are transported in plasma and delivered to recipient cells by high-density lipoproteins. *Nat. Cell Biol.* 2011, 13(4):423–433.

[26] Uzuner E, Ulu GT, Gürler SB, Baran Y. The role of miRNA in cancer: pathogenesis, diagnosis, and treatment. *Methods Mol. Biol.* 2022, 2257:375–422.

[27] Moustafa AA, Kim H, Albeltagy RS, El-Habit OH, Abdel-Mageed AB. MicroRNAs in prostate cancer: From function to biomarker discovery. *Exp. Biol. Med.* 2008, 243(10):817–825.

[28] Mendell JT, Olson EN. MicroRNAs in stress signaling and human disease. *Cell* 2012, 148(6):1172–1187.

[29] Di Leva G, Garofalo M, Croce CM. MicroRNAs in cancer. *Annu. Rev. Pathol.* 2014, 9(1):287–314.

[30] Seok H, Ham J, Jang ES, Chi SW. MicroRNA target recognition: insights from transcriptome-wide non-canonical interactions. *Mol. Cells* 2016, 39(5):375–381.

[31] Peltier HJ, Latham GJ. Normalization of microRNA expression levels in quantitative RT-PCR assays: identification of suitable reference RNA targets in normal and cancerous human solid tissues. *RNA* 2008, 14(5):844–852.

[32] Quang MT, Nguyen MN. The potential of microRNAs in cancer diagnostic and therapeutic strategies: a narrative review. *J Basic Appl Zool.* 2024, 85:1–11.

[33] Lekchnov EA, Amelina EV, Bryzgunova OE, Zaporozhchenko IA, Konoshenko MY, et al. Searching for the novel specific predictors of prostate cancer in urine: The analysis of 84 miRNA expression. *Int. J. Mol. Sci.* 2018, 19(12):4088.

[34] Konoshenko MY, Lekchnov EA, Bryzgunova OE, Kiseleva E, Pyshnaya IA, *et al.* Isolation of extracellular vesicles from biological fluids via the aggregation–precipitation approach for downstream miRNAs detection. *Diagnostics* 2021, 11(3):384.

[35] Lekchnov EA, Zaporozhchenko IA, Morozkin ES, Bryzgunova OE, Vlassov VV, Laktionov PP. Protocol for miRNA isolation from biofluids. *Anal. Biochem.* 2016, 499:78–84.

[36] Chen C, Ridzon DA, Broomer AJ, Zhou Z, Lee DH, *et al.* Real-time quantification of microRNAs by stem–loop RT–PCR. *Nucleic Acids Res.* 2005, 33(20):179.

[37] Boeri M, Verri C, Conte D, Roz L, Modena P, *et al.* MicroRNA signatures in tissues and plasma predict development and prognosis of computed tomography detected lung cancer. *Proc. Natl. Acad. Sci. USA* 2011, 108(9):3713–3718.

[38] Landoni E, Miceli R, Callari M, Tiberio P, Appierto V, *et al.* Proposal of supervised data analysis strategy of plasma miRNAs from hybridisation array data with an application to assess hemolysis-related deregulation. *BMC Bioinform.* 2015, 16:388.

[39] Gantier MP, Sadler AJ, Williams BR, Williams BR. Fine-tuning of the innate immune response by microRNAs. *Immunol. Cell Biol.* 2007, 85(6):458–462.

[40] Anfossi S, Babayan A, Pantel K, Calin GA. Clinical utility of circulating non-coding RNAs – an update. *Nat. Rev. Clin. Oncol.* 2018, 15(9):541–563.

[41] Graveel CR, Calderone HM, Westerhuis JJ, Winn ME, Sempere LF. Critical analysis of the potential for microRNA biomarkers in breast cancer management. *Breast Cancer (Dove Med Press)* 2015, 7:59–79.

[42] Sempere LF, Kauppinen S. Chapter 340 - Translational Implications of MicroRNAs in Clinical Diagnostics and Therapeutics. In *Handbook of Cell Signaling*, 2nd ed. Amsterdam: Elsevier, 2010, pp. 2965–2981.

[43] Konoshenko MY, Lekchnov EA, Bryzgunova OE, Zaporozhchenko IA, Yarmoschuk SV, *et al.* The Panel of 12 Cell-Free MicroRNAs as Potential Biomarkers in Prostate Neoplasms. *Diagnostics.* 2020, 10(1):38.

[44] Porkka KP, Pfeiffer MJ, Waltering KK, Vessella RL, Tammela TL, *et al.* MicroRNA expression profiling in prostate cancer. *Cancer Res.* 2007, 67(13):6130–6135.

[45] Ozen M, Creighton CJ, Ozdemir M, Ittmann M. Widespread deregulation of microRNA expression in human prostate cancer. *Oncogene* 2008, 27:1788-1793.

[46] Luo X, Wen W. MicroRNA in prostate cancer: from biogenesis to applicative potential. *BMC Urol.* 2024, 24(1):244.

[47] Martens-Uzunova ES, Jalava SE, Dits NF, van Leenders GJ, Møller S, *et al.* Diagnostic and prognostic signatures from the small non-coding RNA transcriptome in prostate cancer. *Oncogene.* 2012, 31(8):978–981.

[48] Fabris L, Ceder Y, Chinnaiyan AM, Jenster GW, Sorensen KD, *et al.* The potential of microRNAs as prostate cancer biomarkers. *Eur. Urol.* 2016, 70(2):312–322.

[49] Duca RB, Massillo C, Dalton GN, Farré PL, Graña KD, *et al.* MiR-19b-3p and miR-101-3p as potential biomarkers for prostate cancer diagnosis and prognosis. *Am. J. Cancer Res.* 2021, 11(6):2802–2820.

[50] Santo GD, Frasca M, Bertoli G, Castiglioni I, Cava C. Identification of key miRNAs in prostate cancer progression based on miRNA-mRNA network construction. *Comput. Struct. Biotechnol. J.* 2022, 20(1):864–873.

[51] Zhao J, Xu H, Duan Z, Chen X, Ao Z, *et al.* miR-31-5p regulates 14-3-3 ε to inhibit prostate cancer 22RV1 cell survival and proliferation via PI3K/AKT/Bcl-2 signaling pathway. *Cancer Manag. Res.* 2020, 12:6679–6694.

[52] Mothersill C, Seymour C. Are epigenetic mechanisms involved in radiation-induced bystander effects. *Front. Genet.* 2012, 3:74.

[53] W Zhao, D I Diz, M E Robbins. Oxidative damage pathways in relation to normal tissue injury. *Br. J. Radiol.* 2007, 80(Special Issue 1):S23–S31.

[54] Najafi M, Fardid R, Hadadi G, Fardid M. The mechanisms of radiation-induced bystander effect. *J. Biomed. Phys. Eng.* 2014, 4(4):163–172.

[55] Straub JM, New J, Hamilton CD, Lominska C, Shnayder Y, *et al.* Radiation-induced fibrosis: mechanisms and implications for therapy. *J. Cancer Res. Clin. Oncol.* 2015, 141(11):1985–1994.

[56] Petrović N, Stanojković TP, Nikitović M. MicroRNAs in prostate cancer following radiotherapy: towards predicting response to radiation treatment. *Curr. Med. Chem.* 2022, 29(9):1543–1560.

[57] Malla B, Zaugg K, Vassella E, Aebersold DM, Dal Pra A. Exosomes and exosomal microRNAs in prostate cancer radiation therapy. *Int. J. Radiat. Oncol. Biol. Phys.* 2017, 98(5):982–995.

[58] Ni J, Bucci J, Chang L, Malouf D, Graham P, *et al.* Targeting microRNAs in prostate cancer radiotherapy. *Theranostics* 2017, 7(13):3243–3259.

[59] Matos B, Bostjancic E, Matjasic A, Popovic M, Glavac D. Dynamic expression of 11 miRNAs in 83 consecutive primary and corresponding recurrent glioblastoma: correlation to treatment, time to recurrence, overall survival and MGMT methylation status. *Radiol. Oncol.* 2018, 52(4):422–432.

[60] Barnett GC, West CM, Dunning AM, Elliott RM, Coles CE, *et al.* Normal tissue reactions to radiotherapy: towards tailoring treatment dose by genotype. *Nat. Rev. Cancer* 2009, 9(2):134–142.

[61] Metheetrairut C, Slack FJ. MicroRNAs in the ionizing radiation response and in radiotherapy. *Cancer Genomics* 2013, 23(1):12–19.

[62] Lu C, Zhou D, Wang Q, Liu W, Yu F, *et al.* Crosstalk of microRNAs and oxidative stress in the pathogenesis of cancer. *Oxid. Med. Cell. Longev.* 2020, 2020:2415324.

[63] Mao L, Liu S, Hu L, Jia L, Wang H, *et al.* miR-30 family: A promising regulator in development and disease. *Biomed. Res. Int.* 2018, 2018:9623412.

[64] Zhang Z, Qin H, Jiang B, Chen W, Cao W, *et al.* miR-30e-5p suppresses cell proliferation and migration in bladder cancer through regulating metadherin. *J. Cell Biochem.* 2019, 120(9):15924–15932.

[65] Liu MM, Li Z, Han XD, Shi JH, Tu DY, *et al.* MiR-30e inhibits tumor growth and chemoresistance via targeting IRS1 in breast cancer. *Sci. Rep.* 2017, 7(1):15929.

[66] Ganapathy K, Ngo C, Andl T, Coppola D, Park J, *et al.* Anticancer function of microRNA-30e is mediated by negative regulation of HELLPAR, a noncoding macroRNA, and genes involved in ubiquitination and cell cycle progression in prostate cancer. *Mol. Oncol.* 2022, 16(16):2936–2958.

[67] Wang Y, Zeng G, Jiang Y. The emerging roles of miR-125b in cancers. *Cancer Manag. Res.* 2020, 12:1079–1088.

[68] Zheng Z, Qu JQ, Yi HM, Zhou Y, Wang YY, *et al.* MiR-125b regulates proliferation and apoptosis of nasopharyngeal carcinoma by targeting A20/NF-kappaB signaling pathway. *Cell Death Dis.* 2017, 8(6):e2855.

[69] Mei LL, Wang WJ, Qiu YT, Xie XF, Bai J, *et al.* miR-125b-5p functions as a tumor suppressor gene partially by regulating HMGA2 in esophageal squamous cell carcinoma. *PLoS One* 2017, 12(10):e0185636.

[70] Chen S, Li P, Li J, Zhou L, Wang Y, *et al.* MiR-144 inhibits proliferation and induces apoptosis and autophagy in lung cancer cells by targeting TIGAR. *Cell Physiol. Biochem* 2015, 35(3):997–1007.

[71] Mu Y, Wang Q, Tan L, Lin L, Zhang B. MicroRNA-144 inhibits cell proliferation and invasion by directly targeting TIGAR in esophageal carcinoma. *Oncol. Lett.* 2020, 19(4):3079–3088.

[72] Yao Q, Gu A, Wang Z, Xue Y. MicroRNA-144 functions as a tumor suppressor in gastric cancer by targeting cyclooxygenase-2. *Exp. Ther. Med.* 2018, 15(3):3088–3095.

[73] Sun XB, Chen YW, Yao QS, Chen XH, He M, *et al.* MicroRNA-144 suppresses prostate cancer growth and metastasis by targeting EZH2. *Technol. Cancer Res. Treat* 2021, 20:1533033821989817.

[74] Zheng H, Guo Z, Zheng X, Cheng W, Huang X. MicroRNA-144-3p inhibits cell proliferation and induces cell apoptosis in prostate cancer by targeting CEP55. *Am. J. Transl. Res.* 2018, 10(8):2457–2468.

[75] Matsuzaki J, Suzuki H, Tsugawa H, Watanabe M, Hossain S, *et al.* Bile acids increase levels of microRNAs 221 and 222, leading to degradation of CDX2 during esophageal carcinogenesis. *Gastroenterology* 2013, 145:1300–1311.

[76] Liu K, Li G, Fan C, Diao Y, Wu B, *et al.* Increased expression of microRNA-221 in gastric cancer and its clinical significance. *J. Int. Med. Res.* 2012, 40:467–474.

[77] Matsuzaki J, Suzuki H. Role of MicroRNAs-221/222 in digestive systems. *J. Clin. Med.* 2015, 4(8):1566–1577.

[78] Galardi S, Mercatelli N, Giorda E, Massalini S, Frajese GV, *et al.* MiR-221 and miR-222 expression affects the proliferation potential of human prostate carcinoma cell lines by targeting p27kip1. *J. Biol. Chem.* 2007, 282:23716–23724.

[79] Jia M, Wang Z. MicroRNAs as biomarkers for ionizing radiation injury. *Front. Cell Dev. Biol.* 2022, 10:861451.

[80] Kwak SY, Kim BY, Ahn HJ, Yoo JO, Kim J, Bae IH, *et al.* Ionizing radiation-inducible miR-30e promotes glioma cell invasion through EGFR stabilization by directly targeting CBL-B. *FEBS J.* 2015, 282(8):1512–1525.

[81] Nilsen A, Hillestad T, Skingen VE, Aarnes EK, Fjeldbo CS, *et al.* miR-200a/b/-429 downregulation is a candidate biomarker of tumor radioresistance and independent of hypoxia in locally advanced cervical cancer. *Mol. Oncol.* 2022, 16(6):1402–1419.

[82] Wu W, Chen X, Yu S, Wang R, Zhao R, Du C. MicroRNA-222 promotes tumor growth and confers radioresistance in nasopharyngeal carcinoma by targeting PTEN. *Mol. Med. Rep.* 2018, 17(1):1305–1310.

[83] McGrath J, Kane LE, Maher SG. The influence of MicroRNA-31 on oxidative stress and radiosensitivity in pancreatic ductal adenocarcinoma. *Cells* 2022, 11(15):2294.

[84] Sun T, Yin YF, Jin HG, Liu HR, Tian WC. Exosomal microRNA-19b targets FBXW7 to promote colorectal cancer stem cell stemness and induce resistance to radiotherapy. *Kaohsiung J. Med. Sci.* 2022, 38(2):108–119.

[85] Huang T, Yin L, Wu J, Gu JJ, Wu JZ, *et al.* MicroRNA-19b-3p regulates nasopharyngeal carcinoma radiosensitivity by targeting TNFAIP3/NF-κB axis. *J. Exp. Clin. Cancer Res.* 2016, 35(1):188.

[86] Zaporozhchenko IA, Morozkin ES, Ponomaryova AA, Rykova EY, Cherdyntseva NV, *et al.* Profiling of 179 miRNA expression in blood plasma of lung cancer patients and cancer-free individuals. *Sci. Rep.* 2018, 8(1):6348.

[87] Konoshenko MY, Bryzgunova OE, Laktionov PP. miRNAs and androgen deprivation therapy for prostate cancer. *Biochim. Biophys. Acta Rev. Cancer* 2021, 1876(2):188625.